

# Patterns of growth and the effects of scale on the feeding kinematics of the nurse shark (*Ginglymostoma cirratum*)

Michael P. Robinson\* and Philip J. Motta

Department of Biology, University of South Florida, Tampa, FL 33620, U.S.A.

(Accepted 19 March 2001)

## Abstract

Successful capture of prey often depends, in part, on the magnitude, duration and speed of feeding behaviours. Animal size and experience are potentially important to these aspects of behaviour, but the effects of scale on the muscular dynamics of and capture by aquatic vertebrates remain relatively unknown. This study examines scale effects on prey capture kinematics in the nurse shark *Ginglymostoma cirratum*, an inertial suction feeder. Morphometric analyses were performed on the heads and feeding apparatus of 12 specimens between 71 and 244 cm total length (TL). These data indicated isometric growth of the feeding apparatus. The kinematics of prey capture in another 12 specimens (33 to 268 cm TL) were recorded with high speed video (200 fps). Across the size range, maximal angular excursions remained constant whereas the maxima of linear excursions increased isometrically. However, various phases of the prey capture sequence apparently did not increase in duration. Regressions of the components of prey capture timing generally had slopes between 0 and 0.5, supporting a model of muscular scaling initially proposed for largemouth bass. This model implies that increases in the duration of prey capture are the result of physiological constraints on muscular contraction. There is also a pattern of scaling across several taxa of aquatic vertebrates consistent with a second model of musculoskeletal scaling, although it does not necessarily apply within each taxon.

**Key words:** prey capture, musculoskeletal scaling, Chondrichthyes, nurse shark, kinematics

## INTRODUCTION

Inertial suction feeding, the creation of a sub-ambient pressure in the buccal cavity resulting in the movement of food into the mouth, is the predominant method of prey capture in fishes and is believed to be the ancestral mode of capture for bony fishes (Liem, 1980; Lauder, 1983). The Chondrichthyes share a pre-Devonian ancestor with the Teleostomi (Schaeffer & Williams, 1977; Long, 1995) and exhibit a variety of prey capture methods. An assortment of elasmobranchs uses some degree of inertial suction feeding during prey capture (Motta *et al.*, 2001). Throughout all of these groups of fishes and even within the aquatic amphibians, inertial suction feeding has changed little (Lauder, 1985; Lauder & Prendergast, 1992; Reilly & Lauder, 1992; Reilly, 1995). This lack of change is probably a result of the hydrodynamic constraints of feeding in water (Lauder, 1985) coupled with the necessity for fast movements for

successful prey capture (Alexander, 1967; Muller & Osse, 1978, 1984; Liem, 1980). Fast movements are not only important for capturing evasive prey but are vital to the creation of large amounts of suction (Lauder, 1980; Muller, Osse & Verhagen, 1982; Liem, 1993). Therefore, aspects of an organism's biology that might decrease speed might also decrease prey capture performance. Changes in scale, resulting from ontogenetic growth, can affect kinematics through changes in morphology and/or physiology (Archer, Altringham & Johnston, 1990; Anderson & Johnston, 1992; O'Reilly, Lindstedt & Nishikawa, 1993; Richard & Wainwright, 1995). Subsequently, changes as simple as increases in the size of the mouth or time to open the mouth could affect suction feeding performance. Therefore, the effects of size and scaling are central to a complete understanding of an organism's functional morphology.

The scaling properties of the musculoskeletal system were first discussed in detail a half-century ago (Hill, 1950), but only recently have experimental approaches been used to examine them (Ashley, Reilly & Lauder, 1991; Reilly, 1995; Richard & Wainwright, 1995; Wainwright & Richard, 1995; Wainwright & Shaw,

\*All correspondence to: Department of Biology, P.O. Box 249118, University of Miami, Coral Gables, FL 33124-0421, U.S.A.  
E-mail: michael@fig.cox.miami.edu

1999). The recent work on musculoskeletal dynamics has concentrated on locomotion and aquatic feeding in lower vertebrates, primarily salamanders and bony fishes (Otten, 1983; Ashley *et al.*, 1991; O'Reilly *et al.*, 1993; Ashley-Ross, 1994; Reilly, 1995; Richard & Wainwright, 1995; Hernandez & Motta, 1997; Wainwright & Shaw, 1999). Various patterns of scaling of aquatic feeding have been observed, including cases with no ontogenetic change in feeding kinematics (Hoff, Lannoo & Wassersug, 1985; Reilly, 1995), isometric increases in feeding morphology and function (O'Reilly *et al.*, 1993; Ferry-Graham, 1998b), a combination of isometric and allometric growth in feeding structures and kinematics (Cook, 1996), and isometric increases in feeding morphology and displacements but with decreasing strike durations (Richard & Wainwright, 1995).

Currently, two competing models explain the variation in scaling patterns. One is based on the allometric relationship between the mass of the skeleton and power of the musculature (Hill, 1950; O'Reilly *et al.*, 1993). This model predicts that kinematic velocities should become slower in larger animals, because the power of a muscle decreases relative to the skeletal mass through ontogeny. This model is supported by the feeding kinematics of the toad *Bufo alvarius* (O'Reilly *et al.*, 1993). A second model based on the shortening velocities of muscle fibres argues that with isometric growth and isometry of muscle contraction rates there will be no change in the timing of kinematic events (Richard & Wainwright, 1995). A slight modification of this model incorporating the scaling effects of the dynamics of muscular shortening predicts a slight increase in timing resulting in slopes  $\approx 0.3$  (Richard & Wainwright, 1995). The Richard & Wainwright model, in general, is supported by several taxa of lower vertebrates (Hoff *et al.*, 1985; Reilly, 1995; Richard & Wainwright, 1995; Ferry-Graham, 1998b; Wainwright & Shaw, 1999).

We examine the effects of scale and ontogeny on the feeding kinematics of the nurse shark *Ginglymostoma cirratum* and interpret the results in light of the models of musculoskeletal scaling. Several lines of evidence suggest that elasmobranchs are good models with which to study the effects of scale on aquatic feeding. Unlike the feeding mechanisms of bony fishes, those of cartilaginous fishes consist of relatively few morphological elements that do not undergo radical ontogenetic changes in shape similar to the transition from larva to adult in bony fishes (Bas, 1964; Bass, 1973; Muñoz-Chápuli & Ruiz, 1984; Yano & Musick, 1992; Ellis & Shackley, 1995). The feeding behaviour (Tricas & McCosker, 1984; Tricas, 1985; Strong, Snelson & Gruber, 1990), morphology and mechanics (Springer, 1961; Moss, 1977; Frazzetta & Prange, 1987; Motta, Hueter & Tricas, 1991; Ferry-Graham, 1997, 1998a,b; Motta *et al.*, 1997; Wilga, 1997; Wilga & Motta, 1998a,b; Motta & Wilga, 2001) of elasmobranchs is now quite well studied, including that of the nurse shark *G. cirratum* (Wu, 1994; Motta & Wilga, 1999; Motta *et al.*, 2001). Finally, the nurse shark keeps well in captivity and grows to a large size (*c.* 27 to 304 cm total

length (TL), maturing at 230 cm; Compagno, 1984; Carrier & Luer, 1990) yet remains an obligate suction feeder throughout ontogeny (Tanaka, 1973; Moss, 1977; Motta & Wilga, 1999; Motta *et al.*, 2001). Amongst the specializations for inertial suction feeding, *G. cirratum* possesses reduced teeth, relatively large and reinforced labial cartilages, a small anteriorly directed mouth, large abductor muscles for expanding the orobranchial chamber and the fastest mouth opening recorded for any shark to date (Moss, 1977; Motta & Wilga, 1999; Motta *et al.*, 2001). *Ginglymostoma cirratum* feeds principally on benthic invertebrates (e.g. large gastropods, crustaceans, cephalopods, and sea urchins) and fishes (Bigelow & Schroeder, 1948; Compagno, 1984; Cruz, Díaz & Lalana, 1986; Castro, 2000).

## MATERIALS AND METHODS

### Morphometric data

To test for isometric growth, we recorded the morphometrics of 12 *G. cirratum*. We made external measurements of the head and internal measurements of the feeding skeleton and musculature. We chose the particular internal components of the feeding apparatus based on involvement in the feeding sequence, frequent use in other morphometric studies, or potential to indicate allometry.

The external distances measured were mouth width, internares width, head width at the first gill slit, intereye width (dorsal aspect), distances from the snout to the eye and to the leading edge of the pectoral fin, and the depths of the head at the eye and at the first gill slit. The skeletal elements examined were the upper jaw (palatoquadrate), lower jaw (Meckel's cartilage), and the 3 cartilages of the hyoid arch (the paired hyomandibulae and ceratohyals and the basihyal) (Motta & Wilga, 1999). We measured the mass and greatest length along the longitudinal-axis of each skeletal element; we also measured the height along the dorsal-ventral aspect at mid-length and at the caudal end of the palatoquadrate cartilage (upper jaw) and Meckel's cartilage (lower jaw). The muscles measured were the quadratomandibularis (all divisions combined) and preorbitalis posterior superficial (jaw adductors), coracomandibularis (mandibular depressor), coracohyoideus (hyoid depressor), levator hyomandibularis, levator palatoquadrati proper and the first dorsal constrictor (spiracularis) (hyoid and upper jaw levators) (Motta & Wilga, 1999). We blotted dry all muscles and weighed them; we also measured the cross-sectional area at mid-length of the coracomandibularis and coracohyoideus muscles. We chose to measure cross-sectional area in these 2 muscles, because they are mandibulohyoid abductors that contribute to the generation of the powerful suction forces and because their cylindrical shape and parallel fibres ensured consistent identification of their mid-points. Measurements of mass were to the nearest 0.1 g; linear measurements were made to 0.002 cm. We determined

**Table 1.** *Ginglymostoma cirratum* specimens used in the kinematic analyses of prey capture. All specimens were held in captivity for at least 1 year before experimentation except where noted

Shark number	Total length (cm)	Mass <sup>b</sup> (kg)	Sex	Location	Food species
1	33.0		M	MMA <sup>c</sup>	silverside, <i>Menidia</i> sp.
2 <sup>a</sup>	45.5	0.6	M	MML <sup>d</sup>	herring, <i>Opisthonema oglinum</i>
3 <sup>a</sup>	49.5	0.8	F	MML <sup>d</sup>	<i>O. oglinum</i>
4 <sup>a</sup>	59.0	1.5	F	MML <sup>d</sup>	<i>O. oglinum</i>
5 <sup>a</sup>	63.0	3.0	M	MML <sup>d</sup>	<i>O. oglinum</i>
6	85.0	4.3	M	MML <sup>d</sup>	<i>O. oglinum</i>
7	87.0	4.8	F	MML <sup>d</sup>	<i>O. oglinum</i>
8	93.0	4.3	M	MML <sup>d</sup>	<i>O. oglinum</i>
9	99.1		M	FA <sup>e</sup>	capelin, <i>Mallotus villosus</i>
10	101.6		F	FA <sup>e</sup>	<i>M. villosus</i>
11	211.0	57.0	M	SW <sup>f</sup>	<i>O. oglinum</i> and bonito, <i>Sarda sarda</i>
12	254.0	112.8	F	SW <sup>f</sup>	<i>O. oglinum</i> and <i>S. sarda</i>

<sup>a</sup> Captured in Florida Keys shortly (but at least 5 weeks) prior to start of experimentation.

<sup>b</sup> Mass reported only for those animals weighed shortly before experimentation.

<sup>c</sup> Mote Marine Aquarium: housed in a recirculating exhibit tank; 775 L, S = 35‰ and 24 °C.

<sup>d</sup> Mote Marine Laboratory: housed in exterior tanks with flow-through natural seawater system; 5700 L, 35‰ and *c.* 24 °C.

<sup>e</sup> Florida Aquarium: housed in recirculating exhibit tank with teleosts; 72 000 L, 30‰, and 25 °C.

<sup>f</sup> SeaWorld, Florida: housed in recirculating exhibit tank with teleosts and other large elasmobranchs; 250 000 L, 30‰ and 25 °C.

muscular cross-sectional area by cutting the muscle at its mid-length and digitizing a video image of the cross-section (Sigma Scan Image, Jandel Scientific Software). In the case of paired morphological elements we measured the left element.

### Prey capture kinematics

Twelve different *G. cirratum* were housed at several locations in Florida (Table 1). The animals at Mote Marine Laboratory (MML) and Mote Marine Aquarium (MMA) were fed thrice weekly; all others were fed twice weekly. Filming conditions varied somewhat among the facilities. At MML specimens were starved for 4 to 7 days prior to filming. On days of filming, we placed animals in an observation tank on the same flow-through system as the holding tanks and allowed them at least 45 min to acclimate to the new setting before filming began. This appeared to be ample time, because sharks fed readily and repeatedly. The observation tank (216 cm diameter, 30 cm deep) had 1 flat side of plexiglass (187 cm long) through which feeding was recorded. We filmed the animals at MMA, Florida Aquarium (FA) and Sea World (SW) in the same tanks in which they were housed. They were starved 3 to 6 days before filming. At MMA and SW filming occurred during the regular feeding schedules. In all situations, the sharks fed on food lying freely on the substratum to mimic the natural benthic-feeding style of *G. cirratum*.

We fed the nurse sharks pieces of teleost, because this is their natural prey (Gudger, 1914, 1921; Bigelow & Schroeder, 1948; Compagno, 1984; Castro, 2000) and it constituted their diet prior to these experiments. The food species were the same as those provided during maintenance of the animals (Table 1). The greatest dimension of each piece of food was held constant

relative to the width of the shark's mouth (i.e. maximum food width = 50% of mouth width). Constant relative food size would minimize any possible food-size effects among sharks. When unable to directly measure mouth width (5 sharks among MMA, FA and SW), we estimated it from the following least-squares regression, calculated from 18 *G. cirratum* between 50.5 and 128 cm TL ( $r^2 = 0.722$ , ANOVA:  $P < 0.001$ ):

$$\text{mouth width (cm)} = 0.876 + 0.054 \times (\text{cm TL}).$$

The rate of change of mouth width with total length was quite small (i.e. *c.* 1 cm change in width for every 20 cm change in TL). Therefore, any errors associated with measuring shark length had little consequence on the resulting mouth–food size ratio.

We recorded capture behaviour with a high-speed NAC HSV-200 video camera filming at 200 fields per second (fps) with approximately 3000 watts of illumination. We analysed the kinematics of 5 prey capture events of high intensity for each individual shark. High intensity captures are characterized by very rapid mouth opening and often an audible popping sound during suction, perhaps indicating cavitation (Motta *et al.*, 2001). We defined the start of prey capture ( $t = 0$ ) as the beginning of lower jaw depression and prey ingestion as the time at which the food entered the orobranchial chamber and was no longer visible. We made kinematic analyses of individual video fields beginning 15 ms before and ending 20 ms after completion of the capture attempt, making sure that all components had returned to the state observed before the sequence began.

For kinematic analyses, pertinent individual video fields were captured using a computer-based video capture program. We then used the image analysis program Sigma Scan Image (Jandel Scientific) to record 8 landmarks in each field and used these landmarks to analyse 9 kinematic variables (Fig. 1). Four of the

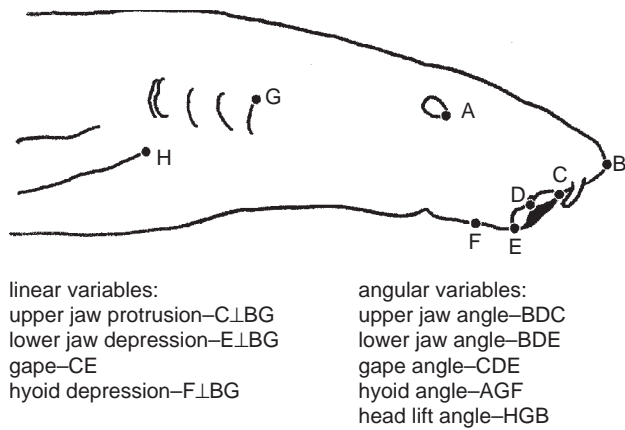


**Fig. 1.** Right lateral view of *Ginglymostoma cirratum* indicating landmarks used to digitize kinematic variables. Landmarks are: A, anterior portion of eye; B, tip of the snout; C, anterior portion of the upper jaw; D, angle of mouth; E, anterior tip of lower jaw; F, location of basihyal cartilage; G, dorsal-most point of first gill slit; H, proximal point of leading edge of pectoral fin. The symbol  $\perp$  indicates this is the segment from the indicated point that intersects perpendicularly with the segment BG.

kinematic variables were linear measurements: gape distance, the distance between points C and E; lower jaw depression distance, the length of the segment that begins at E and intersects perpendicularly to the segment between B and G; upper jaw protrusion distance, the length of the segment originating at C and intersecting perpendicularly with segment BG; hyoid depression distance, the length of the segment originating at point F and intersecting perpendicularly with segment BG. Five kinematic variables were angular: lower jaw depression angle, the angle between points B and E where the centre is point D; upper jaw protrusion angle, the angle between points B and C where the centre is point D; gape angle, the angle between points C and E where the centre is point D; head lift angle, the angle between points H and B where the centre is point G; hyoid depression angle, the angle between points A and F where the centre is point G. We used both the time required to reach maximum value and the maximum values themselves in statistical analyses.

Aside from these kinematic variables, we also calculated the Ram-Suction Index (RSI) for each gape cycle. The RSI is a dimensionless value representing the relative contributions of ram and suction to the prey capture event (Norton & Brainerd, 1993). The RSI represents a point on the continuum between pure ram and pure suction behaviours:

$$RSI = (D_{\text{pred}} - D_{\text{prey}}) / (D_{\text{pred}} + D_{\text{prey}})$$

where  $D_{\text{pred}}$  and  $D_{\text{prey}}$  are the net distances moved by the predator and prey, respectively. In this index, a value of +1 is indicative of a purely ram strike (i.e. movement exclusively by the predator), and a value of -1 is indicative of a purely suction strike (i.e. move-

ment exclusively by the prey). The RSI can lie anywhere from +1 and -1. A value of 0 indicates equal movement of the predator and the prey. We used the eye as the landmark to determine  $D_{\text{pred}}$ .

### Statistical analyses

We log-transformed the scaling data of the morphometric variables and then linearly regressed them against the log TL and log head length (HL—length from snout to anterior margin of pectoral fin) of the shark. We regressed the variables against HL in addition to TL in case the head grew isometrically as a whole but allometrically relative to the rest of the body. In linear variables (e.g. morphometric: length of lower jaw; kinematic: distance of mandibular depression) a slope of 1 would indicate an isometric increase in length or excursion distance. Because of the geometric relationships of length with area and volume (i.e. mass), slopes of 2 for area and 3 for mass are considered isometric, respectively.

We used the Model II geometric mean (GM) regression (Teissier, 1948) for morphometric scaling. We chose this model because the levels of error within the dependent and independent data were nearly equal. In the least squares (LS) regression most of the error should be present in the dependent data. The GM regression is appropriate when levels of error are equal (Ricker, 1973) and is even more robust than LS when considering allometric growth (Ricker, 1984).

We tested each GM regression for statistical significance using its coefficient of correlation ( $r$ ) and the confidence limits of its slope. To test for isometry, we calculated confidence limits for the slopes using the technique of Jolicoeur & Mosimann (1968) and compared them to the isometric values. We then used an iterative procedure by which we calculated the confidence limits of the slopes with successive  $t$ -values until we determined the greatest level of confidence that excluded the isometric slope. This confidence level became the  $P$ -value for the comparison against isometry. For example, if the 94% confidence limits of a regression excluded its isometric slope but the 95% confidence limits did not, then for this comparison with isometry,  $P = 0.06$ . Because of the many simultaneous statistical tests on the different morphometric variables, we applied a sequential Bonferroni correction to the analyses (Rice, 1989). The sequential Bonferroni reduces the experiment-wise error (Type I) but maintains more statistical power than other Bonferroni corrections (Rice, 1989). Statistical power was calculated with the computer program G\*Power (A. Buchner, E. Erdfelder & F. Faul, Heinrich-Heine-Universität, Germany).

Because of the interdependency of the morphometric variables and the loss of power from Bonferroni corrections, we also tested for isometry with a multivariate technique (Bookstein *et al.*, 1985). Briefly, we performed a principal components analysis on the morphometric variables using a covariance matrix. If the variables all

**Table 2.** Scaling relationships of eight external morphometric variables for 12 *Ginglymostoma cirratum*. Geometric mean regressions were determined separately against total and head lengths. Differences from isometric slope (1) were determined by the appropriate confidence limits of the slope. The critical  $P$ -values of these comparisons were sequentially Bonferroni-corrected within total length ( $k = 8$ ) or head length ( $k = 7$ ).  $\alpha_{\text{crit}}$  indicates the probability value required to reject the  $H_0$  of isometry after Bonferroni-corrections;  $\alpha_{\text{calc}}$  represents the probability of that comparison as determined by the confidence limits. The test-wide  $\alpha = 0.05$ . No slope was significantly different from isometry. The power of each analysis ( $1 - \beta$ ) is also indicated. All slopes had 10 df. PCA indicates the loading of the variable on the first principal component with a covariance matrix. These multivariate analyses are independent of total and head lengths

Variable	Total length					Head length					PCA
	Slope	$r^a$	Confidence limits test			Slope	$r^a$	Confidence limits test			
			$\alpha_{\text{crit}}$	$\alpha_{\text{calc}}$	$1 - \beta$			$\alpha_{\text{crit}}$	$\alpha_{\text{calc}}$	$1 - \beta$	
Mouth width	0.860	0.952	0.007	>0.10	0.627	0.940	0.955	0.012	>0.50	0.089	0.152
Internares width	0.860	0.913	0.017	>0.20	0.550	0.940	0.919	0.017	>0.50	0.054	0.146
Head width at 1st gill slit	1.078	0.903	0.050	>0.50	0.077	1.178	0.849	0.050	>0.50	0.145	0.183
Intereye width (dorsal)	0.993	0.957	0.025	>0.50	0.006	1.086	0.936	0.025	>0.50	0.166	0.176
Snout to eye	0.873	0.929	0.010	>0.20	0.455	0.954	0.912	0.008	>0.50	0.045	0.151
Snout to pectoral fin	0.915	0.988	0.006	>0.10	0.283	1.000 <sup>b</sup>					0.167
Head depth at eye	0.861	0.979	0.012	>0.20	0.117	0.941	0.978	0.010	>0.50	0.064	0.158
Head depth at 1st gill slit	0.892	0.955	0.008	>0.20	0.164	0.976	0.949	0.007	>0.50	0.011	0.162

<sup>a</sup> All coefficients of correlation are significant at  $\alpha = 0.01$ .

<sup>b</sup> This slope was calculated from the regression of head length against itself.

load positively and equally onto the first component, the variables are isometric. All variables must be log-transformed and of the same units. Subsequently, the mass, area and linear variables were examined separately; to simplify analyses further, we performed PCA only within similar variables (i.e. external lengths, skeletal lengths, skeletal masses, muscular areas, muscular masses).

We analysed the kinematic data with a LS regression, because it was necessary to compare the kinematic data against the expected slopes of the models (i.e. 0 to 1; see below). Because the slope of the GM regression is determined essentially by a ratio of 2 standard deviations, it can never equal 0 and can only approach 0 asymptotically (Sokal & Rohlf, 1995). Thus, it is not possible to test equally every slope from 0 to 1. More importantly, most of the error is in the dependent data, because the kinematic data probably have a greater proportion of error than the length measurements, making the LS regression appropriate. Finally, the LS regression facilitates comparisons with previous studies (Bennett, Garland & Else, 1989; Archer *et al.*, 1990; Richard & Wainwright, 1995; Wainwright & Shaw, 1999).

We used the kinematic data to examine 3 models of kinematic scaling. All models assume isometric scaling of morphometrics. Subsequently, linear kinematic excursions should scale with a slope of 1 and angular excursions with a slope of 0. However, the models differ in the scaling patterns they predict for the timing variables. The Hill (1950) model predicts timing variables will increase with a slope of 1. The Richard & Wainwright model (1995) predicts that timing will not increase and will have a slope of 0. A modified version of their model predicts a slope of approximately 0.3 (Richard & Wainwright, 1995). If the slopes of the

timing variables do not differ significantly from the slopes predicted by 1 model yet exclude the others, we will argue that the kinematics support that model. We tested each LS regression for statistical significance and used  $t$ -tests to compare their slopes against the expected values. We also applied sequential Bonferroni corrections to the  $t$ -statistics here (Rice, 1989) and calculated statistical power with the program G\*Power.

## RESULTS

### Morphometrics

It appears that the head of *G. cirratum* grows isometrically. Without exception each external morphometric variable was significantly correlated with both total and head length at the 99% level ( $r_{0.99,10\text{df}} = 0.708$ ); none of the slopes of the regressions differed from isometry regardless of whether they were regressed against head or total length (Table 2). Although the Bonferroni corrections resulted in decreased power in many cases, the PCA supports isometry, because all loading values were similar (Table 2).

Internal growth of the feeding apparatus of *G. cirratum* is also mostly isometric. With the exception of basihyal mass (regressed against TL:  $b = 2.405$ ;  $P < 0.05$ ), none of the Bonferroni-corrected skeletal nor muscular variables was allometric (Tables 3 & 4). Values were isometric regardless of whether they were regressed against either TL or HL. The PCA also indicated isometry, because all of the values within each analysis were similar (Tables 3 & 4). The ontogenetic conservation of jaw cartilage shape is illustrated in Fig. 2. All of these isometric relationships were true for both sexes.

**Table 3.** Scaling relationships of skeletal morphometric variables for 12 *Ginglymostoma cirratum*. Geometric mean regressions were calculated *versus* total and head lengths. Differences from the isometric slope were determined by the appropriate confidence limits of the slope. The critical *P*-values of these comparisons were sequentially Bonferroni-corrected within analysis type but across all internal measurements (i.e. total or head length,  $k=22$  for each, see also Table 4).  $\alpha_{crit}$  indicates the probability value required to reject the  $H_0$  of isometry after Bonferroni-corrections;  $\alpha_{calc}$  represents the probability of that comparison as determined by the confidence limits. The effective  $\alpha$  across all internal morphometrics is 0.05. The power of each analysis ( $1-\beta$ ) is also indicated. Slopes differing from isometry are italicized; all had 10 df. PCA indicates the loading of the variable on the first principal component with a covariance matrix. Loading values are comparable only within lengths or masses and are independent of length measure. \*  $P < 0.05$ ; significantly different from isometry when regressed against total length (with sequential Bonferroni-correction) at  $\alpha = 0.05$

Variable	Isometric slope	Total length					Head length					PCA
		Slope	<i>r</i>	Confidence limits test			Slope	<i>r</i>	Confidence limits test			
				$\alpha_{crit}$	$\alpha_{calc}$	$1-\beta$			$\alpha_{crit}$	$\alpha_{calc}$	$1-\beta$	
Upper jaw length	1	1.159	0.888	0.003	>0.30	0.406	1.267	0.862	0.003	>0.20	0.799	0.263
Upper jaw mid-length height	1	0.950	0.879	0.010	>0.50	0.019	1.038	0.845	0.008	>0.50	0.008	0.125
Upper jaw mass	3	2.957	0.960	0.025	>0.50	0.005	3.233	0.947	0.005	>0.40	0.188	0.517
Lower jaw length	1	0.912	0.971	0.002	>0.20	0.696	0.998	0.954	0.05	>0.50	0.002	0.195
Lower jaw mid-length height	1	0.866	0.893	0.003	>0.30	0.515	0.946	0.864	0.006	>0.50	0.024	0.135
Lower jaw caudal height	1	0.922	0.915	0.005	>0.50	0.120	1.008	0.921	0.025	>0.50	0.003	0.167
Lower jaw mass	3	2.700	0.900	0.004	>0.40	0.375	2.951	0.898	0.017	>0.50	0.004	0.517
Hyomandibula length	1	1.057	0.927	0.008	>0.50	0.040	1.155	0.954	0.003	>0.10	0.830	0.193
Hyomandibula mass	3	2.815	0.957	0.004	>0.40	0.228	3.077	0.927	0.01	>0.50	0.009	0.509
Ceratohyal length	1	1.359	0.859	0.002	>0.10	0.891	1.486	0.856	0.002	>0.07	0.809	0.231
Ceratohyal mass	3	2.671	0.938	0.003	>0.20	0.748	2.919	0.933	0.007	>0.50	0.120	0.497
Basihyal length	1	1.159	0.857	0.004	>0.40	0.328	1.267	0.896	0.003	>0.10	0.899	0.255
Basihyal mass	3	2.405	0.987	0.002	<0.002*	0.879	2.629	0.971	0.004	>0.20	0.800	0.468

**Table 4.** Scaling relationships of muscular morphometric variables for 12 *Ginglymostoma cirratum*. Geometric mean regressions were calculated *versus* total and head lengths. Differences from the isometric slope were determined by the appropriate confidence limits of the slope. The critical *P*-values of these comparisons were sequentially Bonferroni-corrected within analysis type but across all internal measurements (i.e. total or head length,  $k=22$  for each, see also Table 3).  $\alpha_{crit}$  indicates the probability value required to reject the  $H_0$  of isometry after Bonferroni-corrections;  $\alpha_{calc}$  represents the probability of that comparison as determined by the confidence limits. The effective  $\alpha$  across all internal morphometrics is 0.05. The power of each analysis ( $1-\beta$ ) is also indicated. No slopes differed from isometry, and all had 10 df. PCA indicates the loading of the variable on the first principal component with a covariance matrix. Loading values are comparable only within areas or masses and are independent of total or head length

Variable	Isometric slope	Total length					Head length					PCA
		Slope	<i>r</i>	Confidence limits test			Slope	<i>r</i>	Confidence limits test			
				$\alpha_{crit}$	$\alpha_{calc}$	$1-\beta$			$\alpha_{crit}$	$\alpha_{calc}$	$1-\beta$	
Coracomandibularis mass	3	3.056	0.922	0.05	>0.50	0.005	3.341	0.908	0.004	>0.40	0.275	0.613
Coracomandibularis cross-sectional area	2	2.174	0.962	0.003	>0.30	0.398	2.376	0.964	0.002	>0.09	0.369	0.401
Coracohyoideus mass	3	2.847	0.946	0.007	>0.50	0.077	3.112	0.904	0.006	>0.50	0.015	0.509
Coracohyoideus cross-sectional area	2	1.855	0.921	0.006	>0.50	0.126	2.028	0.941	0.012	>0.50	0.004	0.348
Levator hyomandibularis mass	3	3.438	0.918	0.003	>0.30	0.793	3.758	0.891	0.003	>0.10	0.892	0.602
Levator palatoquadrati proper mass	3	3.282	0.944	0.004	>0.40	0.366	3.588	0.921	0.003	>0.20	0.757	0.664
1st dorsal constrictor mass	3	3.395	0.961	0.002	>0.20	0.815	3.711	0.943	0.002	>0.09	0.899	0.583
Preorbitalis post. superficial mass	3	3.230	0.935	0.006	>0.50	0.178	3.530	0.929	0.004	>0.20	0.888	0.553
Quadratmandibularis mass	3	3.085	0.920	0.012	>0.50	0.010	3.373	0.911	0.004	>0.40	0.422	0.508

**Table 5.** Scaling relationships of linear and angular excursions for nine kinematic variables for 12 *Ginglymostoma cirratum* (see Table 1). Slopes of least-squares regressions were compared to isometric slopes with sequentially Bonferroni-corrected ( $k = 9$ )  $t$ -tests. Isometry for angular variables is 0, for linear variables is 1.  $\alpha_{crit}$  indicates the probability value required to reject the  $H_0$  of isometry after Bonferroni-corrections;  $\alpha_{calc}$  represents the calculated probability value of that  $t$ -test. The effective  $\alpha$  across all tests is 0.05. The power of each analysis ( $1-\beta$ ) is also indicated. No slopes differed from isometry, and all had 10 df

Variable	Slope	$R$	Comparison vs. isometry		
			$\alpha_{crit}$	$\alpha_{calc}$	$1-\beta$
<b>Maximal angular value</b>					
lower jaw angle	-0.069	0.229	0.010	0.441	0.402
hyoid angle	-0.034	0.167	0.025	0.633	0.229
head lift angle	-0.275	0.324	0.007	0.303	0.652
upper jaw angle	-0.071	0.202	0.017	0.544	0.301
gape angle	-0.118	0.197	0.012	0.536	0.270
<b>Maximal linear excursion</b>					
lower jaw depression	0.941	0.908	0.050	0.693	0.248
hyoid depression	0.870	0.916	0.008	0.308	0.667
upper jaw protrusion	0.750	0.929	0.006	0.024	0.556
gape	0.753	0.877	0.006	0.014	0.326

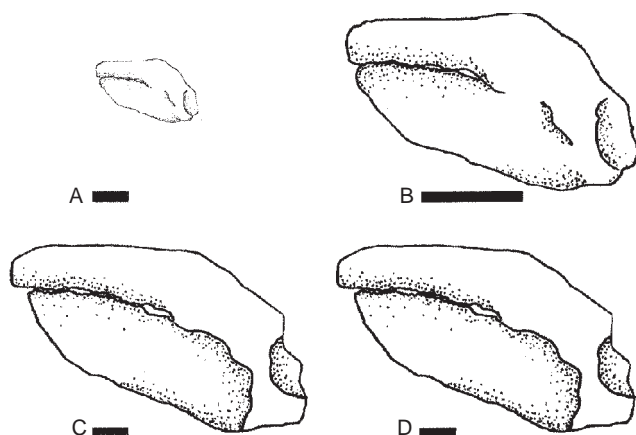


**Fig. 2.** Left lateral view of the upper and lower jaws of two representative *Ginglymostoma cirratum* demonstrating isometric growth of the mandibular arch. Upper shark is 71 cm TL (total length) female; lower individual is 239 cm TL female. A and C are at the same absolute scale. B has been scaled to the same relative length as D to compare better the shapes of the cartilages. Images were traced from video images of jaws. Bars are 2 cm.

### Kinematics

The slopes of the maximal angular variables were not significantly different from 0 (Table 5). In addition, none of the linear kinematic variables regressed against TL differed from the isometric slope of 1. Because the powers of several tests were greater than 0.4 and those tests with slopes most different from isometry had the highest power, it is reasonable to assert that through ontogeny, the maximal angular excursions do not change and the linear excursions increase isometrically.

Although the prey capture sequence appeared to become progressively slower with increasing animal size (Fig. 3, Table 6), only the time to maximal head lift

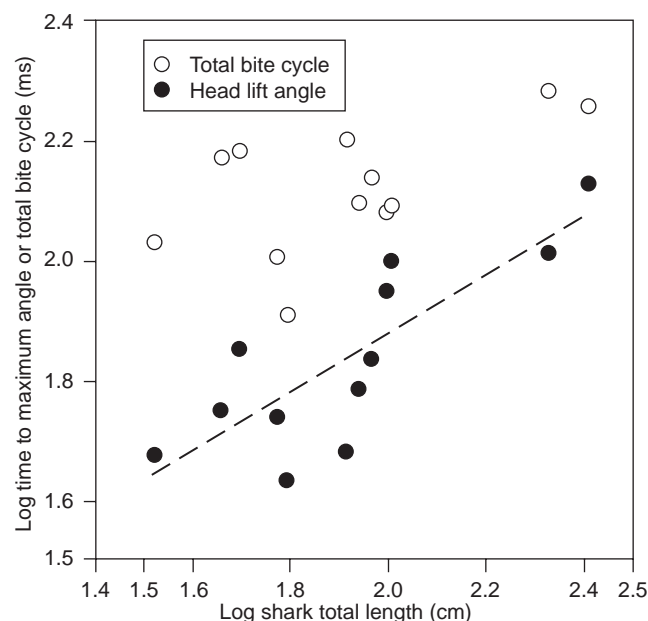


**Fig. 3.** Logarithmic plots of representative kinematic timing variables illustrating the ontogenetic slowing trend of the prey capture sequence for *Ginglymostoma cirratum*. The variables displayed are the mean time to the maximal angle of the head lift and the mean total bite cycle time. The line represents the best-fit, least-squares regression of the head lift angle.

angle differed significantly from 0 (Table 6). Therefore, although the total time to complete the prey capture sequence increased from a mean value of 81 ms in a juvenile 62 cm TL to a maximum mean of 190 ms in an adult 211 cm long (Figs 3 & 4), we could not distinguish its slope of 0.241 from 0. The total bite cycle time and the times to maximum upper jaw angle and gape angle were significantly lower than 1. However, none of the timing variables differed from a slope of 0.3, (Table 6).

**Table 6.** Scaling relationships of the times to maximal excursions of linear and angular kinematic variables for 12 *Ginglymostoma cirratum* (see Table 1). Significance of least square regressions ( $P$ ) was determined by coefficient of correlation ( $r$ ) and ANOVA. Slopes of least-squares regressions were compared to slopes of scaling models with sequentially Bonferroni-corrected ( $k = 18$ )  $t$ -tests.  $\alpha_{crit}$  indicates the probability value required to reject the  $H_0$  of isometry after Bonferroni-corrections;  $\alpha_{calc}$  represents the calculated probability value of that  $t$ -test. The effective  $\alpha$  across all tests is 0.05. The power of each analysis ( $1-\beta$ ) is also indicated. Italicized  $\alpha$ 's indicate which slopes differed from expected values. All slopes had 10 df. \*  $P < 0.05$  after Bonferroni-corrections; \*\*  $P < 0.01$  after Bonferroni-corrections

Variable	Slope	$r$	$P$	vs. 0			vs. 0.3			vs. 1		
				$\alpha_{crit}$	$\alpha_{calc}$	$1-\beta$	$\alpha_{crit}$	$\alpha_{calc}$	$1-\beta$	$\alpha_{crit}$	$\alpha_{calc}$	$1-\beta$
Lower jaw angle	0.396	0.681	0.015	0.005	0.021	0.546	0.010	0.523	0.258	0.004	0.008	0.103
Hyoid angle	0.405	0.577	0.049	0.008	0.492	0.357	0.012	0.575	0.215	0.004	0.008	0.116
Head lift angle	0.484	0.812	0.001	0.003	<i>0.002*</i>	0.896	0.007	0.233	0.834	0.004	0.005	0.071
Upper jaw angle	0.344	0.669	0.017	0.004	0.017	0.492	0.025	0.722	0.131	0.003	<i>&lt;0.001**</i>	0.876
Gape angle	0.333	0.593	0.042	0.006	0.041	0.350	0.050	0.821	0.113	0.003	<i>&lt;0.001*</i>	0.892
Total cycle time	0.241	0.580	0.048	0.006	0.048	0.341	0.017	0.594	0.227	0.003	<i>&lt;0.001**</i>	0.880

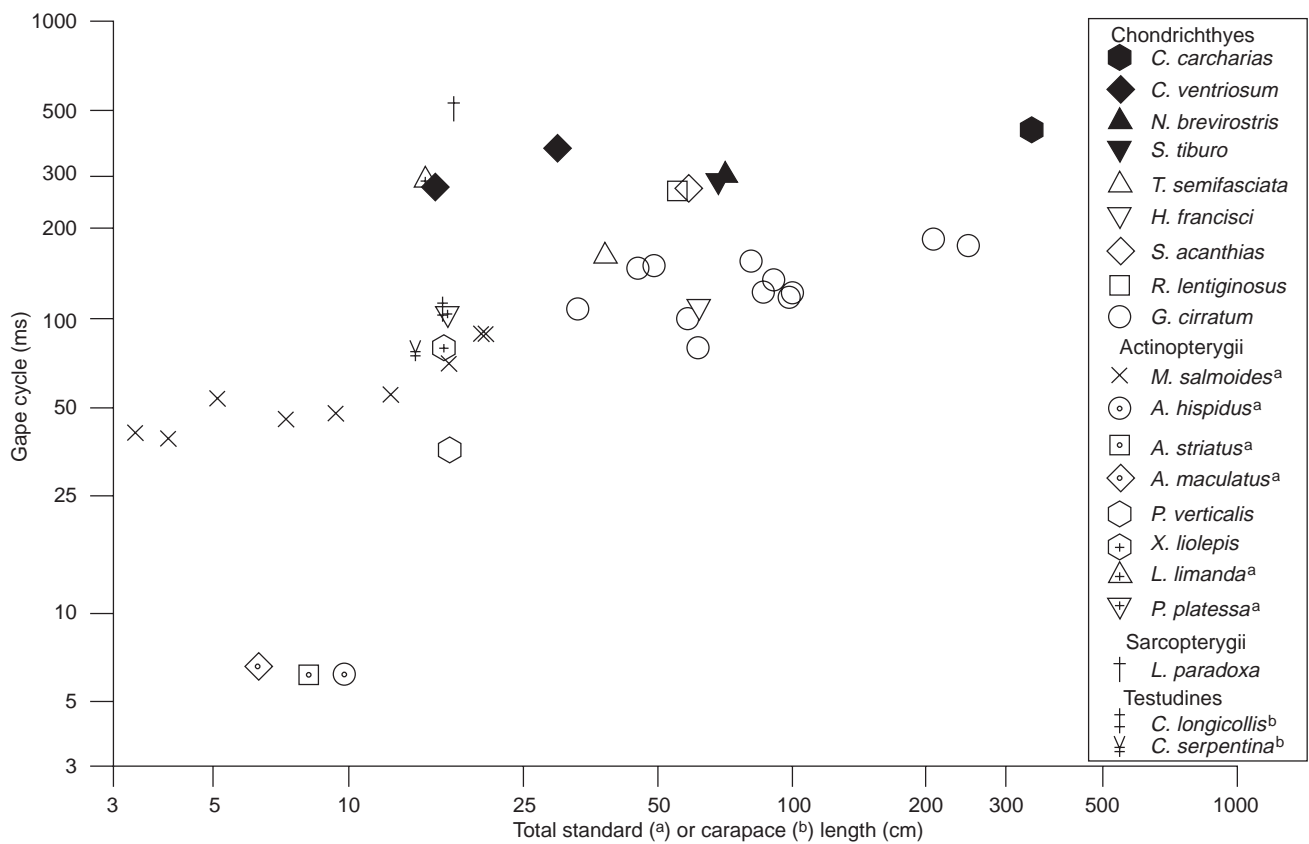


**Fig. 4.** Plots of durations of prey capture cycle for several species of aquatic vertebrates (see Table 8 for full list). Points represent reported mean values for length and prey capture duration except in *Micropterus salmoides* (all data for 10 bass), *Cephaloscyllium ventriosum* (means of two size classes), and *Ginglymostoma cirratum* (data from this study). Chondrichthyes with filled symbols are primarily ram feeders; those with open symbols are primarily suction feeders. The Y-axis depicts the time to complete prey capture. The X-axis is animal total length except where noted: a, standard length; b, carapace length. Note logarithmic axes.

The RSI did not change through ontogeny, either (Table 7). Suction, as indicated by a negative RSI, was the primary means by which food was captured regardless of shark size. The regression of RSI against TL resulted in a very small and non-significant coefficient of correlation ( $r = -0.209$ , 10 df,  $P = 0.515$ ). The mean

RSI of each shark ranged from  $-0.554$  to  $-0.241$ , but there was no significant difference among the individuals (Kruskal-Wallis one-way ANOVA on Ranks:  $H = 8.439$ , 11 df,  $P = 0.674$ ). The lowest (i.e. most suction-based) overall value was  $-0.958$ , whereas the highest was  $0.428$ , a range of  $1.387$ , but 58 of the 60

**Table 7.** Mean Ram-Suction Index (RSI) values for prey capture in 12 *Ginglymostoma cirratum*. Negative values indicate captures that include a higher percentage of suction than ram

Shark total length	RSI	SEM	Minimum	Maximum
33.0	-0.446	0.106	-0.680	-0.049
45.5	-0.276	0.135	-0.754	-0.012
49.5	-0.542	0.080	-0.782	-0.302
59.0	-0.476	0.095	-0.675	-0.196
62.0	-0.496	0.131	-0.781	-0.091
85.0	-0.240	0.172	-0.547	0.428
87.0	-0.377	0.179	-0.958	0.172
92.0	-0.289	0.087	-0.619	-0.104
99.1	-0.483	0.125	-0.904	-0.160
101.6	-0.398	0.119	-0.824	-0.097
211.0	-0.463	0.140	-0.818	0.000
254.0	-0.554	0.064	-0.733	-0.405

total prey capture events had RSI values less than 0. The overall mean RSI was  $-0.420$ , which was significantly less than 0 (two-tailed  $t$ -test:  $t = 12.000$ , 59 df,  $P < 0.001$ ).

## DISCUSSION

### Isometry of the feeding mechanism

The feeding apparatus of *G. cirratum* grows isometrically. Of the 53 morphometric regressions scaled against TL and HL, only one differed significantly from isometry (Tables 2, 3 & 4). Although in many cases the statistical power was low, thus decreasing our likelihood of detecting significant differences, the low power was most common when the calculated slope was quite close to its predicted value. Such a situation produces a small effect size which results in the low statistical power. Because the low power was primarily a result of the closeness between the calculated and predicted slopes, we propose that this indicates isometry regardless of the statistical power. In addition, multivariate analyses indicated that variation among the morphometric variables was quite equitable, implying isometry. Given these isometric conditions, it seems likely that the biomechanical qualities of the feeding apparatus do not change throughout ontogeny. These data do not necessarily predict a lack of ontogenetic physiological change, but they do imply that there will probably be no change in kinematics resulting directly from changes in the biomechanics of the feeding mechanism. However, this presumes constancy in lever mechanics.

Isometry of the head of *G. cirratum* is somewhat surprising considering that allometry is relatively common in elasmobranchs. Although external isometry of the head has been observed in at least a few species of elasmobranchs (Bass, 1973; Ferry-Graham, 1998b), many species from several orders exhibit allometry of the head (Bas, 1964; Bass, 1973; Muñoz-Chápuli &

Ruiz, 1984; Yano & Musick, 1992; Ellis & Shackley, 1995). Other than heterodonty (Raschi, Musick & Compagno, 1982; Kajiura & Tricas, 1996), internal allometry of the head has not yet been reported in elasmobranchs, although it is implied by allometry in some external measurements (Bas, 1964; Bass, 1973; Muñoz-Chápuli & Ruiz, 1984; Yano & Musick, 1992; Ellis & Shackley, 1995). At present, however, it appears that the entire head of *G. cirratum* grows isometrically relative to the length of the body and as a unit unto itself.

### Kinematic scaling

The kinematic excursions of prey capture in *G. cirratum* are isometric. Maximal angular excursions did not change ontogenetically, and the linear variables increased at slopes not different from 1 (Table 5). These kinematic results, in conjunction with the morphometrics, suggest that the feeding apparatus of *G. cirratum* not only grows isometrically but also its function does not change ontogenetically. Similar results were found for the prey capture kinematics of the fire salamander *Salamandra salamandra* (only angular variables measured; Reilly, 1995), and the large-mouth bass *Micropterus salmoides* (Richard & Wainwright, 1995).

Although the kinematic excursions of *G. cirratum* increased isometrically, three of the timing variables had slopes significantly less than 1 (Table 6). In addition, although the kinematic timing variables were greatest with the largest sharks, only five of the six slopes differed from 0. However, none of the slopes differed significantly from 0.3.

### Comparison to scaling models

In general, the kinematics of *G. cirratum* support the scaling model of Richard & Wainwright (1995). This model argues that scaling patterns are dependent on the contractile dynamics of individual muscle fibres. In this model the rate of shortening per sarcomere does not change ontogenetically, but the fibres added linearly by growth result in the linear addition of their shortening velocities. Thus, a longer muscle will contract more quickly and over a greater absolute length, but it will contract the same relative length in the same time. Therefore, assuming isometry of growth and muscular contraction rates, there will be no change in the times to kinematic maxima (i.e.  $b = 0$ ). Richard & Wainwright (1995) modified their model by adding an ontogenetic increase in times of muscular contraction (Marsh, 1988; Bennett *et al.*, 1989; Archer *et al.*, 1990). This modification results in predicted slopes equal to those observed in the scaling of fibre contraction (i.e.  $b = c$ . 0.3). An alternative model predicts isometric increases in the slopes of timing variables (Hill, 1950; O'Reilly, *et al.*, 1993). The power of a muscle, directly related to its area (Asmussen, 1962; Close, 1972), scales with a slope of 2,

whereas the mass of the skeleton increases at a slope of 3. Thus, through ontogeny, the power of the muscle decreases relative to the mass it must move, and kinematic velocities become slower in larger animals. The Hill model predicts increases ( $b=1$ ) in the times to reach kinematic maxima. The kinematics of *B. alvarius*, *S. salamandra*, *Ambystoma maculatum*, and *Cephaloscyllium ventriosum* support this model (Hoff *et al.*, 1985; O'Reilly *et al.*, 1993; Reilly, 1995; Ferry-Graham, 1998b).

The times to maxima and the prey capture duration of *G. cirratum* all scaled with slopes from 0.241 to 0.484, values very similar to those predicted by the modified Richard & Wainwright model. Only one of these slopes differed significantly from 0 (i.e. head lift angle,  $b=0.484$ ), and none differed from the slope of 0.3 predicted by the unmodified Richard & Wainwright model. Three of the six slopes differed from 1, which is the slope predicted by the Hill model. Therefore, the feeding kinematics of *G. cirratum* appear to favour the Richard & Wainwright model over the Hill model. The trends supporting the modified Richard & Wainwright model would probably become significant if more specimens were included in the analyses, as indicated by the strong coefficients of correlation. The trends are likely to be real but obscured by inter-individual variation as demonstrated by the relatively low statistical power. Inter-individual variation is common in the feeding kinematics of elasmobranchs (Tricas & McCosker, 1984; Motta *et al.*, 1997; Wilga, 1997; Wilga & Motta, 1998a; Edmonds, 1999) and teleosts (e.g. Wainwright & Shaw, 1999) and probably played a role in the low coefficients of correlation. None the less, this study, along with that of Richard & Wainwright (1995), provides good support for their model of prey capture scaling, although it cannot easily distinguish between the original and modified versions. If the scaling of prey capture kinematics of *G. cirratum* does correspond to the modified Richard & Wainwright model, the muscular contractile properties of *G. cirratum* probably scale to body size with negative allometry as assumed in that model and observed in other lower vertebrates (Marsh, 1988; Bennett *et al.*, 1989; Archer *et al.*, 1990). However, further research into the scaling of muscular contraction would be necessary.

### Suction, speed and scaling

As indicated by the RSI results and previous studies (Tanaka, 1973; Moss, 1977; Motta *et al.*, 2001), the nurse shark feeds principally by suction. It has many of the morphological and kinematic specializations associated with suction feeding (Lauder, 1980; Muller *et al.*, 1982; Liem, 1993), including a small, laterally enclosed gape, reduced dentition, large, rapid buccal expansion and peak hyoid depression after peak gape (Motta *et al.*, 2001). The relative amounts of suction and ram feeding, as indicated by the RSI, did not change over the size range studied. We did not measure suction

directly, and RSI only indicates the relative rather than absolute amounts of suction and ram. While there is some evidence that the absolute value of suction does increase (Tanaka, 1973), the relative values of suction and ram did not change. This is in contrast to prey capture in juvenile swell sharks *C. ventriosum*, where hatchlings had a larger component of ram in their strikes than 1-year-old sharks (Ferry-Graham, 1998b). This change was attributed to their inexperience and the functional effects of their smaller buccal cavities (Ferry-Graham, 1998b). However, use of suction by newborn *G. cirratum* might differ from the smallest juveniles used here (c. 1-year-old). None the less, these data imply that the relative contribution of suction to prey capture does not change ontogenetically in post-hatchling *G. cirratum*, an obligate suction feeder. There is a great change in buccal cavity size over the size range examined, but, unlike *C. ventriosum*, this apparently does not result in an effect on the suction of *G. cirratum*, probably as a result of its other specializations for suction feeding.

Fast feeding movements are crucial not only for capturing elusive prey but also in the generation of large amounts of suction. With the statistical power of these tests, it was not possible to detect an increase in the duration of prey capture kinematics in *G. cirratum* with increasing animal size. Even if total bite cycle does increase, as implied by the more than doubling in time from the slowest shark to the largest (i.e. 81 to 190 ms), this difference might not be ecologically meaningful. It is impossible to say that scale would have no effect on prey capture performance without tests of performance, but some data suggest that it has a minimal effect if any. Despite possible increases in prey capture times, there is no obvious change in the prey of *G. cirratum* with ontogeny (Gudger, 1914, 1921; Bell & Nichols, 1921; Beebe & Tee-Van, 1928; Bigelow & Schroeder, 1948; Compagno, 1984; Cruz *et al.*, 1986; Castro, 2000). In addition, the benthic prey of *G. cirratum* (e.g. small eels and other fishes, lobsters, gastropods) are probably more susceptible to the greater suction generated by larger sharks (Tanaka, 1973). Therefore, it appears that any slowing of prey capture by larger *G. cirratum* would not decrease its feeding performance.

The nurse shark has a faster prey capture cycle than any elasmobranch studied thus far, including those that use inertial suction feeding (Fig. 4; Motta *et al.*, 2001). Among the elasmobranchs, only three sharks, all of them suction-feeders, approach the speed of *G. cirratum*: *Heterodontus francisci*, *Triakis semifasciata* and *Squalus acanthias*. The elasmobranchs that primarily use ram feeding (i.e. *Carcharodon carcharias*, *Cephaloscyllium ventriosum*, *Negaprion brevirostris* and *Sphyrna tiburo*) have slower prey capture sequences than the suction feeders (i.e. *T. semifasciata*, *H. francisci*, *S. acanthias*, *Rhinobatos lentiginosus* and *G. cirratum*), and there is little overlap between the groups (Table 8). Again, this is probably a result of the necessity of rapid feeding behaviours to generate subambient pressures (Lauder, 1980; Muller *et al.*, 1982; Liem, 1993).

**Table 8.** Species used in the analyses of the intertaxonomic scaling relationships of aquatic prey capture in vertebrates

Taxon	Length (cm) <sup>a</sup>	Bite cycle (ms)	Source
<b>Chondrichthyes</b>			
<i>Carcharodon carcharias</i> , white shark	350	443	Tricas, 1985 Tricas & McCosker, 1984
<i>Cephaloscyllium ventriosum</i> , swellshark	15.8, 30.0	280, 360 <sup>d</sup>	Ferry-Graham, 1998 <sup>b</sup>
<i>Ginglymostoma cirratum</i> , nurse shark	33–254	81–190 <sup>d</sup>	Current study
<i>Heterodontus francisci</i> , horn shark	63	113 <sup>e</sup>	Edmonds, 1999
<i>Negaprion brevirostris</i> , lemon shark	72	309	Motta <i>et al.</i> , 1997
<i>Rhinobatos lentiginosus</i> , Atlantic guitarfish	56.5	274	Wilga & Motta, 1998 <sup>b</sup>
<i>Squalus acanthias</i> , spiny dogfish	59	280	Wilga & Motta, 1998 <sup>a</sup>
<i>Sphyrna tiburo</i> , bonnethead shark	69	302	Wilga, 1997
<i>Triakis semifasciata</i> , leopard shark	38	165	Ferry-Graham, 1998 <sup>a</sup>
<b>Actinopterygii</b>			
<i>Antennarius hispidus</i> , splitlure frogfish	9.8 <sup>b</sup>	6.3	Grobecker & Pietsch, 1979, T. Pietsch, pers. comm.
<i>A. striatus</i> , striated frogfish	8.2 <sup>b</sup>	6.2	Grobecker & Pietsch, 1979, T. Pietsch, pers. comm.
<i>A. maculatus</i> , clown frogfish	6.3 <sup>b</sup>	6.7	Grobecker & Pietsch, 1979, T. Pietsch, pers. comm.
<i>Micropterus salmoides</i> , largemouth bass	3.3–20.6 <sup>b</sup>	38–89 <sup>d</sup>	Richard & Wainwright, 1995 P. C. Wainwright, pers. comm.
<i>Pleuronichthys verticalis</i> , hornyhead turbot	17	36	Gibb, 1995
<i>Xytreurys liolepis</i> , fantail sole	16.5	79.7	Gibb, 1996
<i>Pleuronectes platessa</i> , plaice	16.8 <sup>b,e</sup>	103.5	Bels & Davenport, 1996
<i>Limanda limanda</i> , dab	15.0 <sup>b,e</sup>	293.6	Bels & Davenport, 1996
<b>Sarcopterygii</b>			
<i>Lepidosiren paradoxa</i> , lungfish	17.5	521.5 <sup>f</sup>	Bemis & Lauder, 1986
<b>Testudines</b>			
<i>Chelodina longicollis</i> , snake-necked turtle	16.5 <sup>c</sup>	110	Van Damme & Aerts, 1997
<i>Chelydra serpentina</i> , snapping turtle	14.2 <sup>c</sup>	78.1 <sup>f</sup>	Lauder & Prendergast, 1992

<sup>a</sup> Lengths given in total length (TL) except where noted.

<sup>b</sup> Standard length (SL).

<sup>c</sup> Carapace length (CL).

<sup>d</sup> Analysed as a single mean value.

<sup>e</sup> For unattached prey only.

<sup>f</sup> Mode of lengths.

<sup>g</sup> Calculated from four individuals in published figure.

<sup>h</sup> For fish prey only.

Although there are differences among the elasmobranchs, their overall trend of prey capture is similar to that observed across a number of aquatic vertebrates (Fig. 4, Table 8). There is a significant relationship between animal size and prey capture duration spanning the largemouth bass *M. salmoides* (3.3 cm SL), and anglerfishes *Antennarius* (6.3 cm SL), to the white shark *Carcharodon carcharias* (350 cm TL) (LS regression:  $n = 20$ ,  $a = 0.649$ ,  $b = 0.949$ ,  $r = 0.684$ ,  $P < 0.001$ ). This slope is greater than that seen in the scaling of muscular contraction (i.e.  $c. 0.3$ :  $t = 2.715$ , 18 df,  $P < 0.02$ ; Marsh, 1988; Bennett *et al.*, 1989; Archer *et al.*, 1990; Anderson & Johnston, 1992) and is not significantly different from 1 ( $t = 0.213$ ,  $P > 0.5$ ). The pattern is possibly the result of musculoskeletal dynamics as predicted by the Hill (1950) model whereby skeletal mass increases at a greater rate than muscular power.

In addition to a common scaling pattern across all of these aquatic vertebrates, there appear to be unique scaling factors at work within and among species. As a group the non-elasmobranch fishes reveal no significant scaling relationship ( $n = 9$ ,  $r = 0.797$ ,  $P = 0.010$ ,  $1 - \beta = 0.923$ ), but each of *Micropterus salmoides*, *Lepomis macrochirus*, and *L. punctatus* has a significant relation-

ship (Richard & Wainwright, 1995; Wainwright & Shaw, 1999). Common scaling factors act across all taxa and determine the slope of the higher-level taxonomic groupings. Examples of common factors would include the constraints of muscle-physiology such as a slowing of muscle shortening rate with increasing size (Archer *et al.*, 1990) or possibly the allometric relationship between muscle power and skeletal mass as predicted by Hill (1950). The unique factors would be taxon-specific and depend on the level of taxonomic analysis (e.g. species vs. order). These scaling factors might depend on the feeding architecture and behaviour of each group. For example, allometry in one taxon and isometry in another sister taxon would be two unique factors that would cause differences in scaling relationships. The regressions of these two groups would have different slopes and/or intercepts, although they might be similar in a larger context. Based on the common scaling factor(s), an animal's size would determine its position in the overall scaling relationship (Fig. 4, both horizontal and vertical location). The specific pattern of scaling within that group would depend on its unique scaling factor(s).

In conclusion, the feeding apparatus of *G. cirratum*

grows isometrically. The kinematic excursions of the prey capture sequence were isometric. The duration of prey capture kinematics generally support a modified scaling model of Richard & Wainwright (1995) although the slight increase in timing with size was not significant. The relationship, however, between the feeding kinematics and size of *G. cirratum* differs from the very strong trend observed across all aquatic vertebrates. This disparity is likely to be a result of unique scaling factors that differ among taxa (e.g. different feeding architectures). There do appear to be some common scaling factors that affect scaling patterns across taxa, the most likely being the scaling of muscular contraction (Archer *et al.*, 1990) or the relationship between muscle power and skeletal mass as predicted by Hill (1950). None the less, any possible increase in prey capture times in *G. cirratum* at the levels believed to occur would be of little ecological consequence to this obligate suction feeder.

### Acknowledgements

We would like to thank R. Hueter and H. Mushinsky for ideas and discussion. Reviews by them, S. Maciá, P. Wainwright and two anonymous reviewers greatly improved the manuscript. C. Luer, Mote Marine Lab, R. Davis, SeaWorld, and the Florida Aquarium generously provided specimens to film. J. Castro, NMFS, and the Keys Marine Lab provided some specimens for dissection. P. Wainwright and T. Pietsch graciously provided unpublished data. M. Edmonds, A. Griffith, K. Overholtzer, H. Porter, D. Sasko, T. Streelman, and C. Wilga assisted with discussion and data collection. MPR was supported primarily by The Mote Marine Lab and University of South Florida Fellowship in Elasmobranch Biology. The project was partially supported by a National Science Foundation grant (DEB 9117371) to PJM.

### REFERENCES

- Alexander, R. M. (1967). *Functional design in fishes*. London: Hutchinson & Co., Ltd.
- Anderson, E. M. & Johnston, I. A. (1992). Scaling of power output in fast muscle fibres of the Atlantic cod during cyclical contractions. *J. exp. Biol.* **170**: 143–154.
- Archer, S. D., Altringham, J. D. & Johnston, I. A. (1990). Scaling effects on the neuromuscular system, twitch kinetics and morphometrics of the cod, *Gadus morhua*. *Mar. Behav. Physiol.* **17**: 137–146.
- Ashley, M. A., Reilly, S. M. & Lauder, G. V. (1991). Ontogenetic scaling of hindlimb muscles across metamorphosis in the tiger salamander, *Ambystoma tigrinum*. *Copeia* **1991**: 767–776.
- Ashley-Ross, M. A. (1994). Metamorphic and speed effects on hindlimb kinematics during terrestrial locomotion in the salamander *Dicamptodon tenebrosus*. *J. exp. Biol.* **193**: 285–305.
- Asmussen, E. (1962). Muscular performance. In *Muscle as a tissue*: 161–175. Rodahl, K. & Horvath, S. M. (Eds). New York: McGraw-Hill Book Company, Inc.
- Bas, C. (1964). Aspectos del crecimiento relativo de *Scylliorhinus canicula*. *Inv. Pesq.* **27**: 3–12.
- Bass, A. J. (1973). Analysis and description of variation in the proportional dimensions of scylliorhinid, carcharhinid and sphyrnid sharks. *S. Afr. Assoc. Mar. Biol. Oceanogr. Res. Rep.* **32**: 1–28.
- Beebe, W. & Tee-Van, J. (1928). The fishes of Port-Au-Prince, Haiti. *Zoologica* **10**: 1–279.
- Bell, J. C. & Nichols, J. T. (1921). Notes on the food of Carolina sharks. *Copeia* **1921**: 17–20.
- Bels, V. L. & Davenport, J. (1996). A comparison of food capture and ingestion in juveniles of two flatfish species, *Pleuronectes platessa* and *Limanda limanda* (Teleostei: Pleuronectiformes). *J. Fish Biol.* **49**: 390–401.
- Bemis, W. E. & Lauder, G. V. (1986). Morphology and function of the feeding apparatus of the lungfish, *Lepidosiren paradoxa* (Dipnoi). *J. Morphol.* **187**: 81–108.
- Bennett, A. F., Garland, T., Jr. & Else, P. L. (1989). Individual correlation of morphology, muscle mechanics, and locomotion in a salamander. *Am. J. Physiol.* **256**: R1200–R1208.
- Bigelow, H. B. & Schroeder, W. C. (1948). *Fishes of the western North Atlantic. Part I. Lancelets, cyclostomes, sharks*. Memoirs of the Sears Foundation of Marine Research.
- Bookstein, F. L., Chernoff, B., Elder, R. L., Humphries, J. M., Smith, G. R. & Strauss, R. E. (1985). *Morphometrics in evolutionary biology*. Special Publication 15. Philadelphia: Academy of Natural Sciences.
- Carrier, J. C. & Luer, C. A. (1990). Growth rates in the nurse shark, *Ginglymostoma cirratum*. *Copeia* **1990**: 686–692.
- Castro, J. I. (2000). The biology of the nurse shark, *Ginglymostoma cirratum*, off the Florida east coast and the Bahama Islands. *Environ. Biol. Fish.* **58**: 1–22.
- Close, R. I. (1972). Dynamic properties of mammalian skeletal muscles. *Physiol. Rev.* **52**: 129–197.
- Compagno, L. J. V. (1984). FAO species catalogue, *Sharks of the world. An annotated and illustrated catalogue of shark species known to date*. Part 1. *Hexanchiformes to Lamniformes*. **4**. FAO Fish. Synop.
- Cook, A. (1996). Ontogeny of feeding morphology and kinematics in juvenile fishes: a case study of the cottid fish *Clinocottus analis*. *J. exp. Biol.* **199**: 1961–1971.
- Cruz, R., Díaz, E. & Lalana, R. (1986). Ecología de la langosta (*Panulirus argus*) al SE de la Isla de la Juventud. I. Colonización de arrecifes artificiales. *Rev. Invest. Mar.* **7**: 3–17.
- Edmonds, M. A. (1999). *Prey capture kinematics in the horn shark, Heterodontus francisci*. MS thesis, University of South Florida, Tampa.
- Ellis, J. R. & Shackley, S. E. (1995). Ontogenetic changes and sexual dimorphism in the head, mouth and teeth of the lesser spotted dogfish. *J. Fish Biol.* **47**: 155–164.
- Ferry-Graham, L. A. (1997). Feeding kinematics of juvenile swellsharks, *Cephaloscyllium ventriosum*. *J. exp. Biol.* **200**: 1255–1269.
- Ferry-Graham, L. A. (1998a). Effects of prey size and mobility on prey-capture kinematics in leopard sharks *Triakis semifasciata*. *J. exp. Biol.* **201**: 2433–2444.
- Ferry-Graham, L. A. (1998b). Feeding kinematics of hatchling swellsharks, *Cephaloscyllium ventriosum* (Scylliorhinidae): the importance of predator size. *Mar. Biol.* **131**: 703–718.
- Frazzetta, T. H. & Prange, C. D. (1987). Movements of cephalic components during feeding in some requiem sharks (Carcharhiniformes: Carcharhinidae). *Copeia* **1987**: 979–993.
- Gibb, A. C. (1995). Kinematics of prey capture in a flatfish, *Pleuronichthys verticalis*. *J. exp. Biol.* **198**: 1173–1183.
- Gibb, A. C. (1996). Kinematics of prey capture in *Xystreurys hiolepis*: do all flatfish feed asymmetrically? *J. exp. Biol.* **199**: 2269–2283.
- Grobecker, D. B. & Pietsch, T. W. (1979). Hi-speed cinematographic evidence for ultrafast feeding in antennariid anglerfishes. *Science (Washington)* **205**: 1161–1162.

- Gudger, E. W. (1914). The nurse sharks of Boca Grande Key, Florida. *Science (Washington)* **40**: 386.
- Gudger, E. W. (1921). Notes on the morphology and habits of the nurse shark, *Ginglymostoma cirratum*. *Copeia* **1921**: 57–59.
- Hernandez, L. P. & Motta, P. J. (1997). Trophic consequences of differential performance: ontogeny of oral jaw-crushing performance in the sheepshead, *Archosargus probatocephalus* (Teleostei, Sparidae). *J. Zool. (Lond.)* **243**: 737–756.
- Hill, A. V. (1950). The dimensions of animals and their muscular dynamics. *Sci. Prog. (Lond.)* **38**: 209–230.
- Hoff, K. S., Lannoo, M. J. & Wassersug, R. J. (1985). Kinematics of midwater prey capture by *Ambystoma* (Caudata: Ambystomatidae). *Copeia* **1985**: 247–251.
- Jolicoeur, P. & Mosimann, J. E. (1968). Intervalles de confiance pour la pente de l'axe majeur d'une distribution normale bidimensionnelle. *Biometrie-Praximetrie* **9**: 121–140.
- Kajiura, S. M. & Tricas, T. C. (1996). Seasonal dynamics of dental sexual dimorphism in the Atlantic stingray *Dasyatis sabina*. *J. exp. Biol.* **199**: 2297–2306.
- Lauder, G. V. (1980). Evolution of the feeding mechanism in primitive actinopterygian fishes: a functional anatomical analysis of *Polypterus*, *Lepisosteus*, and *Amia*. *J. Morphol.* **163**: 283–317.
- Lauder, G. V. (1983). Food capture. In *Fish biomechanics*: 280–311. Webb, P. W. & Weihs, D. (Eds). New York: Praeger Publishers.
- Lauder, G. V. (1985). Aquatic feeding in lower vertebrates. In *Functional morphology*: 210–229. Hildebrand, M., Bramble, D. M., Liem, K. F. & Wake, D. B. (Eds). Cambridge, MA: Harvard University Press.
- Lauder, G. V. & Prendergast, T. (1992). Kinematics of aquatic prey capture in the snapping turtle *Chelydra serpentina*. *J. exp. Biol.* **164**: 55–78.
- Liem, K. F. (1980). Acquisition of energy by teleosts: adaptive mechanisms and evolutionary patterns. In *Environmental physiology of fishes*: 299–334. Ali, M. A. (Ed.). New York: Plenum Publishing Corp.
- Liem, K. F. (1993). Ecomorphology of the teleostean skull. In *The skull. Functional and evolutionary mechanisms*: 422–452. Hanken, J. & Hall, B. K. (Eds). Chicago: University of Chicago Press.
- Long, J. A. (1995). *The rise of fishes*. Baltimore: John Hopkins University Press.
- Marsh, R. L. (1988). Ontogenesis of contractile properties of skeletal muscle and sprint performance in the lizard *Dipsosaurus dorsalis*. *J. exp. Biol.* **137**: 119–139.
- Moss, S. A. (1977). Feeding mechanisms in sharks. *Am. Zool.* **17**: 355–364.
- Motta, P. J., Hueter, R. E. & Tricas, T. C. (1991). An electromyographic analysis of the biting mechanism of the lemon shark, *Negaprion brevirostris*: functional and evolutionary implications. *J. Morphol.* **210**: 55–69.
- Motta, P. J., Hueter, R. E., Tricas, T. C. & Summers, A. P. (2001). A kinematic analysis of suction feeding in the nurse shark, *Ginglymostoma cirratum* (Orectolobiformes, Ginglymostomatidae). *Copeia* **2001**: 24–38.
- Motta, P. J., Tricas, T. C., Hueter, R. E. & Summers, A. P. (1997). Feeding mechanism and functional morphology of the jaws of the lemon shark *Negaprion brevirostris* (Chondrichthyes, Carcharhinidae). *J. exp. Biol.* **200**: 2765–2780.
- Motta, P. J. & Wilga, C. A. D. (1999). Anatomy of the feeding apparatus of the nurse shark, *Ginglymostoma cirratum*. *J. Morphol.* **241**: 33–60.
- Motta, P. J. & Wilga, C. A. D. (2001). Advances in the study of feeding behaviors, mechanisms, and mechanics of sharks. *Environ. Biol. Fishes* **60**: 131–156.
- Muller, M. & Osse, J. W. M. (1978). Structural adaptations to suction feeding in fish. *Proc. Zodiac Symp. on Adaptation*. Wageningen, The Netherlands.
- Muller, M. & Osse, J. W. M. (1984). Hydrodynamics of suction feeding in fish. *Trans. zool. Soc. Lond.* **37**: 51–135.
- Muller, M., Osse, J. W. M. & Verhagen, J. H. G. (1982). A quantitative hydrodynamic model of suction feeding in fishes. *J. Theor. Biol.* **95**: 49–79.
- Muñoz-Chápuli, R. & Ruiz, M. B. (1984). Tendencias generales del crecimiento relativo en escualos. *Inv. Pesq.* **48**: 303–317.
- Norton, S. F. & Brainerd, E. L. (1993). Convergence in the feeding mechanics of ecomorphologically similar species in the Centrarchidae and Cichlidae. *J. exp. Biol.* **176**: 11–29.
- O'Reilly, J. C., Lindstedt, S. L. & Nishikawa, K. C. (1993). The scaling of feeding kinematics in toads (Anura: Bufonidae). *Am. Zool.* **33**: 147A.
- Otten, E. (1983). The jaw mechanism during growth of a generalized *Haplochromis* species: *H. elegans* Trewavas 1933 (Pisces, Cichlidae). *Neth. J. Zool.* **33**: 55–98.
- Raschi, W., Musick, J. A. & Compagno, L. J. V. (1982). *Hypoprion bigelowi*, a synonym of *Carcharhinus signatus* (Pisces: Carcharhinidae), with a description of ontogenetic heterodonty in this species and notes on its natural history. *Copeia* **1982**: 102–109.
- Reilly, S. M. (1995). The ontogeny of aquatic feeding behavior in *Salamandra salamandra*: stereotypy and isometry in feeding kinematics. *J. exp. Biol.* **198**: 701–708.
- Reilly, S. M. & Lauder, G. V. (1992). Morphology, behavior, and evolution: comparative kinematics of aquatic feeding in salamanders. *Brain Behav. Evol.* **40**: 182–196.
- Rice, W. R. (1989). Analyzing tables of statistical tests. *Evolution* **43**: 223–225.
- Richard, B. A. & Wainwright, P. C. (1995). Scaling the feeding mechanism of largemouth bass (*Micropterus salmoides*): kinematics of prey capture. *J. exp. Biol.* **198**: 419–433.
- Ricker, W. E. (1973). Linear regressions in fishery research. *J. Fish. Res. Bd. Can.* **30**: 409–434.
- Ricker, W. E. (1984). Computation and uses of central trend lines. *Can. J. Zool.* **62**: 1897–1905.
- Schaeffer, B. & Williams, M. (1977). Relationships of fossil and living elasmobranchs. *Am. Zool.* **17**: 293–302.
- Sokal, R. R. & Rohlf, F. J. (1995). *Biometry*. New York: W. H. Freeman & Comp.
- Springer, S. (1961). Dynamics of the feeding mechanism of large galeoid sharks. *Am. Zool.* **1**: 183–185.
- Strong, W. R., Jr., Snelson, F. F. & Gruber, S. H. (1990). Hammerhead shark predation on stingrays: an observation of prey handling by *Sphyrna mokarran*. *Copeia* **1990**: 836–840.
- Tanaka, S. K. (1973). Suction feeding by the nurse shark. *Copeia* **1973**: 606–608.
- Teissier, G. (1948). La relation d'allométrie: sa signification statistique et biologique. *Biometrics* **4**: 14–43.
- Tricas, T. C. (1985). Feeding ethology of the white shark, *Carcharodon carcharias*. *Mem. So. Calif. Acad. Sci.* **9**: 81–91.
- Tricas, T. C. & McCosker, J. E. (1984). Predatory behavior of the white shark (*Carcharodon carcharias*), with notes on its biology. *Proc. Calif. Acad. Sci.* **43**: 221–238.
- Van Damme, J. & Aerts, P. (1997). Kinematics and functional morphology of aquatic feeding in Australian snake-necked turtles (Pleurodira: *Chelodina*). *J. Morphol.* **233**: 113–125.
- Wainwright, P. C. & Richard, B. A. (1995). Scaling the feeding mechanism of the largemouth bass (*Micropterus salmoides*): motor patterns. *J. exp. Biol.* **198**: 1161–1171.
- Wainwright, P. C. & Shaw, S. S. (1999). Morphological basis of kinematic diversity in feeding sunfishes. *J. exp. Biol.* **202**: 3101–3110.
- Wilga, C. A. D. (1997). *Evolution of feeding mechanisms in elasmobranchs: a functional morphological approach*. PhD thesis, University of South Florida, Tampa.
- Wilga, C. A. D. & Motta, P. J. (1998a). Conservation and variation in the feeding mechanism of the spiny dogfish *Squalus acanthias*. *J. exp. Biol.* **201**: 1345–1358.

- Wilga, C. A. D. & Motta, P. J. (1998b). Feeding mechanism of the Atlantic guitarfish *Rhinobatos lentiginosus*: modulation of kinematic and motor activity. *J. exp. Biol.* **201**: 3167–3184.
- Wu, E. H. (1994). Kinematic analysis of jaw protrusion in orectolobiform sharks: a new mechanism for jaw protrusion in elasmobranchs. *J. Morphol.* **222**: 175–190.
- Yano, K. & Musick, J. A. (1992). Comparison of morphometrics of Atlantic and Pacific specimens of the false catshark, *Pseudotriakis microdon*, with notes on stomach contents. *Copeia* **1992**: 877–886.